

# SPACE-TIME CONSERVATION METHOD APPLIED TO NUMERICAL SOLUTION OF WATER HAMMER EQUATIONS

KATARZYNA WEINEROWSKA-BORDS

*Faculty of Civil and Environmental Engineering,  
Gdansk University of Technology,  
Narutowicza 11/12, 80-233 Gdansk, Poland  
kwein@pg.gda.pl*

(Received 27 June 2011; revised manuscript received 10 September 2011)

**Abstract:** This paper is devoted to the space-time conservation (STC) method and its application to a water hammer in steel pipelines. The STC method, due to its numerical properties, in particular its high accuracy, can be an interesting alternative to traditional numerical methods, especially when dealing with problems where the numerical errors have the potential to significantly influence the solution, making interpretation very difficult. As the problem of water hammer is one of such problems, an analysis of the application of the STC method to this case can be very interesting.

**Keywords:** water hammer, unsteady flow in pipelines, numerical methods, numerical dissipation

## 1. Introduction

A water hammer consists in violent changes of pressure values in the form of a rapid pressure wave, which occurs in a pipeline as a consequence of sudden changes in flow velocity. The celerity of such a disturbance is a function of the liquid compressibility and elasticity of the pipe walls and may exceed 1000 m/s. Unfortunately, the pressure oscillates between very high and very low values (sometimes leading to underpressure) with a high frequency, which means that the phenomenon may become particularly dangerous, despite being short-lived.

A traditional description of a water hammer in a pipeline was given by Allievi [1, 2] and its subsequent modifications are due to Jaeger [3], Wood [4], Parmakian [5], Streeter and Lai [6], Streeter and Wylie [7], and Chaundry [8]. The relationships between the basic parameters of pressurized water flow during rapid

unsteady conditions may be derived from the mass and momentum conservation equations, and can be expressed as a set of two hyperbolic equations:

$$\frac{1}{\rho a^2} \frac{\partial p}{\partial t} + \frac{v}{\rho A^2} \frac{\partial p}{\partial x} + \frac{\partial v}{\partial x} = 0 \quad (1a)$$

$$\frac{\partial v}{\partial t} + v \frac{\partial v}{\partial x} + \frac{1}{\rho A} \frac{\partial(\beta-1)\rho v^2 A}{\partial x} = -g \sin \theta - \frac{1}{\rho} \frac{\partial p}{\partial x} - \frac{\tau_s O_z}{\rho A} \quad (1b)$$

where  $p$  and  $v$  are, respectively, the mean values of pressure and flow velocity in the pipe cross-section,  $\rho$  is the density of the liquid,  $g$  is the acceleration due to gravity,  $a$  is the pressure wave celerity,  $A$  is the cross-section area,  $\beta$  is the Saint-Venant coefficient,  $\theta$  is the angle between the pipe axis and the horizontal,  $O_z$  is the wetted perimeter,  $\tau_s$  is the shear stress, and  $x$  and  $t$  denote the distance and time variable, respectively.

The above system of equations is often simplified by neglecting the terms whose values are very small in comparison with the remaining terms. As in the case of a water hammer the Mach number satisfies  $Ma \ll 1$ , Equations (1) can be simplified to the following form:

$$\frac{1}{\rho a^2} \frac{\partial p}{\partial t} + \frac{v}{\rho A^2} \frac{\partial p}{\partial l} + \frac{\partial v}{\partial l} = 0 \quad (2a)$$

$$\frac{\partial v}{\partial t} + \frac{1}{\rho} \frac{\partial p}{\partial l} + g \sin \theta + \frac{\tau_s \pi D}{\rho A} = 0 \quad (2b)$$

It is more convenient to perform calculations in terms of the water head rather than pressure, the above equations can be further rewritten to this end. Following the application of the Darcy-Weisbach formula, we obtain a system of equations often considered to be the classical description of a water hammer (*e.g.* [5]):

$$\frac{\partial v}{\partial t} + v \frac{\partial v}{\partial x} + g \frac{\partial H}{\partial x} + \frac{\lambda}{2D} v |v| = 0 \quad (3a)$$

$$\frac{\partial H}{\partial t} + v \frac{\partial H}{\partial x} + \frac{a^2}{g} \frac{\partial v}{\partial x} = 0 \quad (3b)$$

where  $D$  is the internal diameter of the pipe, and  $\lambda$  is a linear friction factor. The description of a water hammer defined by Equation (2) or (3) is valid for 1D flows of compressible fluids in deformable pipes, as long as the Mach number ( $Ma$ ) satisfies  $Ma \ll 1$ .

The above systems of equations can be solved using numerical modeling. The most popular approaches applied to the solution of the water hammer problem are the method of characteristics (MOC) and various finite difference methods (FDMs), the finite volume method (FVM) can also be applied. Since the comparison of the calculated results and the measurements showed a significant discrepancy, attempts were made at modifying the system of equations. Many authors focused on improving the shear stress in (1) or (2) (*e.g.* [9–13]). This, however, did not lead to satisfactory results, as apparent good agreement resulted from the influence of significant numerical errors, not from a proper mathematical description of the phenomenon [14]. The results of calculations are easier to

interpret when a highly accurate numerical scheme is applied and an analysis of accuracy and stability is carried out.

An interesting alternative to the commonly applied numerical methods for solving partial differential equations (MOC, FDM, FVM) is the non-traditional approach proposed by Chang [15]. This method is relatively new and rarely used. Originally, this approach was known as the *method of space-time conservation element and solution element*, however, in this paper we refer to it as the *space-time conservation* (STC) method. The calculations in the STC approach are performed on the basis of enforcement of flux conservation (which is also the basic assumption of the finite volume method) with the unification of space and time, which are treated on an equal footing. Such an approach leads to the construction of space-time cells (or in the case of 1D problems – rectangles in the  $x-t$  plane), in which flux conservation is enforced.

The STC method, previously applied to solving classical initial-boundary problems of the Saint-Venant equations [16], constitutes a modification of a scheme called “ $a - \mu$ ” [15], which was originally applied to solving the advection-diffusion equation. It was shown previously [17] that the STC method can be also successfully applied to solving the reverse flow routing problem. In the next section, the application of the STC method to the water hammer problem is presented.

## 2. Solution of a system of water hammer equations using the STC method

The application of the STC method requires that the description of the analyzed problem expressed as a system of equations is written in conservative form. Such a description helps to avoid many difficulties which arise during the computations when the non-conservative form of the equations is used, *e.g.* those related to mass conservation.

A system of equations describing a water hammer (2), combined with the Darcy-Weisbach friction formula, is rewritten for a horizontal pipe in its conservation form:

$$\frac{\partial \mathbf{f}}{\partial t} + \frac{\partial \mathbf{G}}{\partial x} = \mathbf{S} \quad (4a)$$

where

$$\mathbf{f} = \begin{Bmatrix} p \\ q \end{Bmatrix}, \quad \mathbf{G} = \begin{Bmatrix} \frac{q^2}{A} \\ \frac{q^2}{\rho A} + Ap \end{Bmatrix}, \quad \mathbf{S} = \begin{Bmatrix} 0 \\ -\frac{\lambda g |q|}{2\rho AD} \end{Bmatrix} \quad (4b)$$

where  $q = \rho v A$ .

Assuming elastic behavior of water and of the pipe wall material, the density of water and the cross-section area can be defined as follows:

$$\rho = \rho_o \left( 1 + \frac{p - p_o}{E_c} \right) \quad (5)$$

$$A = A_o \left( 1 + \frac{D}{e} \frac{p - p_o}{E_s} \right) \quad (6)$$

where  $D$  is the internal diameter of the pipe,  $e$  is the pipe wall thickness,  $E_s$  is the modulus of elasticity of the pipe wall, and  $E_c$  is the bulk modulus of the fluid. The

subscript “o” in (5) and (6) denotes values under steady-flow conditions, *i.e.* the density, pressure and the pipe cross-section, respectively. The wave celerity  $a$ , can be expressed with the Moens-Korteweg equation [18]:

$$a = \sqrt{\frac{E_c}{\rho} \left(1 + \frac{DE_c}{e E_s}\right)^{-1}} \quad (7)$$

According to the assumptions of the STC method, the solution of (4) is sought in 2D space-time  $(x, t)$ .

Let the solution domain in the global case be an area  $\Omega$  with the boundary  $s(\Omega)$  (Figure 1). For this area, flux conservation through the boundary is enforced and Equations (4) must be satisfied. Thus, the integral is calculated as follows:

$$\iint_{\Omega} \left( \frac{\partial \mathbf{f}}{\partial t} + \frac{\partial \mathbf{G}}{\partial x} \right) d\Omega = \iint_{\Omega} \mathbf{S} d\Omega \quad (8)$$

The left-hand side of Equation (8) can be transformed by applying Green’s theorem [19]:

$$\iint_{\Omega} \left( \frac{\partial \mathbf{f}}{\partial t} + \frac{\partial \mathbf{G}}{\partial x} \right) d\Omega = \oint_{s(\Omega)} \mathbf{f} dx - \mathbf{G} dt = \oint_{s(\Omega)} \mathbf{h} ds \quad (9)$$

where  $\mathbf{h} = (\mathbf{G}, \mathbf{f})$ , and  $\mathbf{h} ds$  represents the space-time flux of  $\mathbf{h}$  through  $s(\Omega)$ . The integration along the boundary of the domain  $\Omega$  is performed anticlockwise.

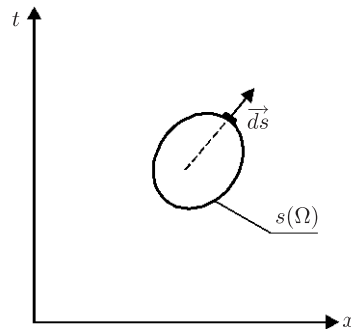


Figure 1. Solution domain in the  $x$ - $t$  plane

By applying Equation (9) to Equation (8), the integral form of Equation (3a) is obtained:

$$\oint_{s(\Omega)} \mathbf{h} ds = \oint_{s(\Omega)} \mathbf{f} dx - \mathbf{G} dt = \iint_{\Omega} \mathbf{S} d\Omega \quad (10)$$

An uncommon unification of variables  $x$  and  $t$  is proposed, and the integration is performed along the  $s(\Omega)$  curve in the  $(x, t)$  plane. Such an approach is considerably different from those of other methods, including the finite volume method, which operate on volumes in geometric space.

The solution domain for the water hammer problem can be represented by a plane shown in Figure 2. The plane is covered with a set of nodal points  $(j, n)$  described by indices  $j = 1, 2, \dots, M$  and  $n = 0, 1, \dots, N$  (Figure 2, panel (a)). The grid constructed in such a way is additionally covered by a set of intermediate points in a staggered mesh, with indices  $(j \pm 1/2, n \pm 1/2)$  for  $j = 2, 3, \dots, M - 1$  and  $n = 2, 3, \dots, N - 1$ . Consequently, a grid as in Figure 2, panel (a) is obtained. The values in the nodes at the time level  $n$  are known. The unknown values at the cross-section  $n + 1$  are calculated in two stages. First, the values in the intermediate points at the time level  $n + 1/2$  are computed, then, according to the same formulas, the step from  $n + 1/2$  to  $n$  is made.

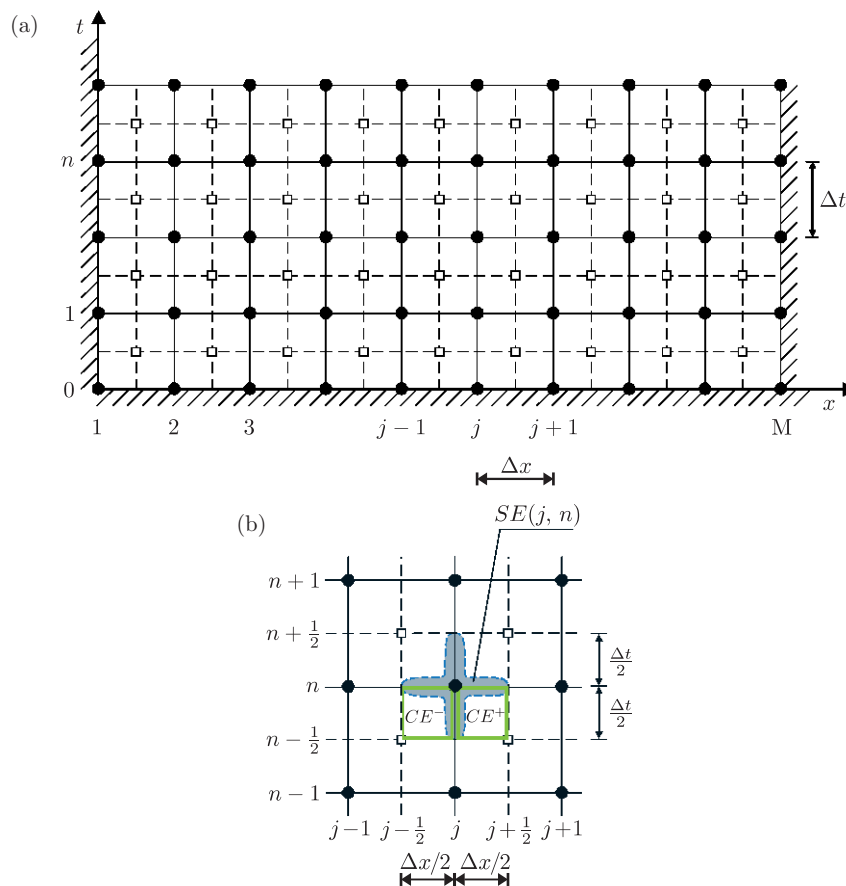


Figure 2. (a) Mesh of nodes in the STC method; (b) solution element  $SE(j, n)$  and conservation elements  $CE^-$  and  $CE^+$

Equation (10) must be satisfied in the whole solution domain  $\Omega$ , which is equivalent to global flux conservation. Moreover, local flux conservation is also required in each cell comprising the solution domain. The cells, termed *conservation elements (CEs)*, are rectangular domains of the dimensions  $\Delta x/2$

and  $\Delta t/2$  in the  $(x, t)$  plane. Each cell is defined by two nodes of the grid, situated on the diagonal of the rectangle (Fig. 2, panel b). In order to determine the values of  $\mathbf{f}$  and  $\mathbf{G}$  in each cell, a *solution element* ( $SE$ ) is defined around every mesh point of the grid. Every  $SE$  consists of vertical and horizontal segments of the grid (of the lengths of  $\Delta x/2$  and  $\Delta t/2$ , respectively), going from the mesh point in question in the positive and negative directions of the  $x$  and  $t$  axes to the nearest neighbours of these segments. An example of an  $SE$  corresponding to the node  $(j, n)$  is shown in Figure 2, panel (b).

In each solution element, for any  $(x, t) \in SE(j, n)$  the values of  $\mathbf{f}$  and  $\mathbf{G}$  are approximated by  $\mathbf{f}^*$  and  $\mathbf{G}^*$ , according to:

$$\mathbf{f}^*(x, t; j, n) = \mathbf{f}_j^n + (\mathbf{f}_x)_j^n (x - x_j) + (\mathbf{f}_t)_j^n (t - t^n) \quad (11a)$$

$$\mathbf{G}^*(x, t; j, n) = \mathbf{G}_j^n + (\mathbf{G}_x)_j^n (x - x_j) + (\mathbf{G}_t)_j^n (t - t^n) \quad (11b)$$

where,  $\mathbf{f}_j^n$ ,  $(\mathbf{f}_x)_j^n$ ,  $(\mathbf{f}_t)_j^n$  and  $\mathbf{G}_j^n$ ,  $(\mathbf{G}_x)_j^n$ ,  $(\mathbf{G}_t)_j^n$ , respectively, are the constants in  $SE(j, n)$ ; and  $(x_j, t^n)$  are the coordinates of the node  $(j, n)$ . From Equations (11), it follows that:

$$\mathbf{f}^*(x_j, t^n; j, n) = \mathbf{f}_j^n \quad (12a)$$

$$\frac{\partial \mathbf{f}^*}{\partial x}(x_j, t^n; j, n) = (\mathbf{f}_x)_j^n, \quad \frac{\partial \mathbf{f}^*}{\partial t}(x_j, t^n; j, n) = (\mathbf{f}_t)_j^n \quad (12b, c)$$

and similarly for  $\mathbf{G}$ .

The values of variables  $\mathbf{f}_j^n$ ,  $(\mathbf{f}_x)_j^n$  and  $(\mathbf{f}_t)_j^n$  in Equation (11a) are the values of the function  $\mathbf{f}$  and its derivatives  $\partial \mathbf{f} / \partial x$  and  $\partial \mathbf{f} / \partial t$  in the node  $(j, n)$  (similarly for  $\mathbf{G}$  – from Equation (11b)). Thus, the right-hand side expressions in Equations (11) become first-order Taylor series expansions of  $\mathbf{f}$  and  $\mathbf{G}$  around the node  $(j, n)$ . The values of  $\mathbf{f}_j^n$ ,  $(\mathbf{f}_x)_j^n$  and  $(\mathbf{f}_t)_j^n$  can be treated as numerical equivalents of  $\mathbf{f}$  and its derivatives  $\partial \mathbf{f} / \partial x$  and  $\partial \mathbf{f} / \partial t$  (and similarly for  $\mathbf{G}$ ) in the node  $(j, n)$ . Moreover,  $\mathbf{f} = \mathbf{f}^*(x, t; j, n)$  and  $\mathbf{G} = \mathbf{G}^*(x, t; j, n)$  should satisfy Equation (3a), which implies that:

$$(\mathbf{f}_t)_j^n = \mathbf{S}_j^n - (\mathbf{G}_x)_j^n \quad (13)$$

Any segment that constitutes a side of the  $CE$  (e.g. segment AB in Figure 3, panel (b)) is also an interface separating two adjoining cells (e.g.  $CE^-(j, n)$  and  $CE^+(j, n)$ ). The flux through this interface is evaluated using information from only one  $SE$  ( $SE(j, n)$ ).

In each cell flux must be conserved. The values of  $\mathbf{f}$  and  $\mathbf{G}$  for each cell are approximated by  $\mathbf{f}^*$  and  $\mathbf{G}^*$ , according to formulas (11a) and (11b) for suitable  $SE$ s, which constitute the cell boundary. Since the boundary of each cell is composed of the segments that belong to two neighbouring  $SE$ s, the values of only two nodes, i.e. one at the “known” (lower) and one at the “unknown” (higher) time level, appear in the conservation equation for each cell.

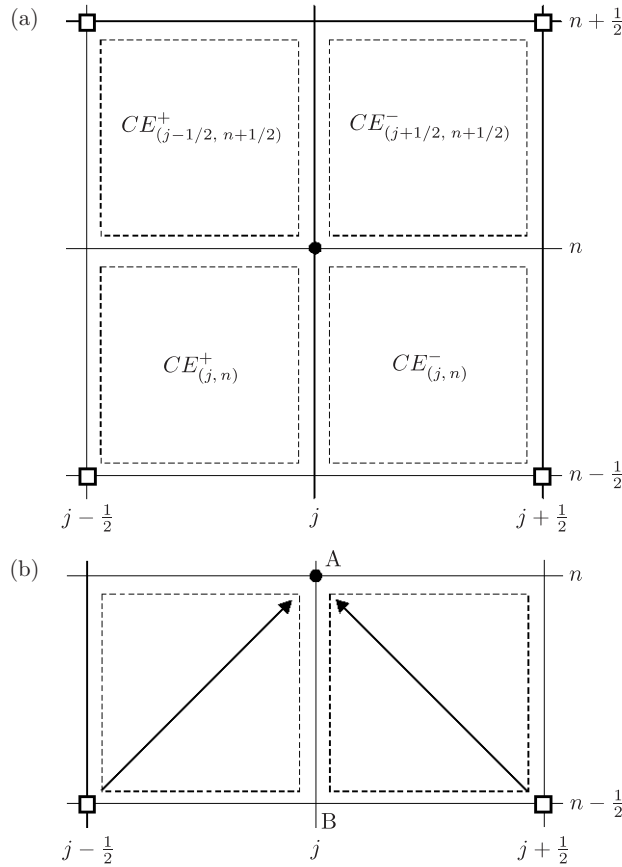


**Figure 3.** (a) Conservation cells associated with  $SE(j,n)$ ; (b) Conservation cells influencing the value of functions  $f$  and  $G$  in the node  $(j,n)$

Let the variables at the time level  $n - 1/2$  be known, whereas the variables at the time level  $n$  are sought. Moreover, let:

$$F^+(j,n) = \oint_{s(CE^+_{(j,n)})} -G^* dt + f^* dx = F^+ \quad (14a)$$

$$F^-(j,n) = \oint_{s(CE^-_{(j,n)})} -G^* dt + f^* dx = F^- \quad (14b)$$

By substituting Eqsations (11) into Equations (14) and by integrating along the boundary of  $CE^+(j,n)$  and  $CE^-(j,n)$ , we obtain:

$$\frac{2}{\Delta x} F^+ = f_j^n + \frac{\Delta x}{4} (f_x)_j^n - \frac{\Delta t}{\Delta x} G_j^n + \frac{(\Delta t)^2}{4\Delta x} (G_t)_j^n - f_{j+1/2}^{n-1/2} + W_{j+1/2}^{n-1/2} \quad (15a)$$

$$\frac{2}{\Delta x} F^- = f_j^n - \frac{\Delta x}{4} (f_x)_j^n + \frac{\Delta t}{\Delta x} G_j^n - \frac{(\Delta t)^2}{4\Delta x} (G_t)_j^n - f_{j-1/2}^{n-1/2} + W_{j-1/2}^{n-1/2} \quad (15b)$$

where

$$\mathbf{W}_{j\pm 1/2}^{n-1/2} = \frac{\Delta x}{4} (\mathbf{f}_x)_{j\pm 1/2}^{n-1/2} + \frac{\Delta t}{\Delta x} \mathbf{G}_{j\pm 1/2}^{n-1/2} + (\mathbf{G}_t)_{j\pm 1/2}^{n-1/2} \frac{(\Delta t)^2}{4\Delta x} \quad (15c)$$

We note that

$$\mathbf{G}_t = \frac{\partial \mathbf{G}}{\partial t} = \frac{\partial \mathbf{G}}{\partial \mathbf{f}} \frac{\partial \mathbf{f}}{\partial x} = \frac{\partial \mathbf{G}}{\partial \mathbf{f}} \mathbf{f}_x \quad (16)$$

which means that the fluxes  $F^+$  and  $F^-$  from Equation (15) can be expressed as a combination of  $\mathbf{f}$ ,  $\mathbf{G}$  and  $\mathbf{f}_x$ .

According to Equation (10), it is required that:

$$F^+ = \iint_{\Omega(CE^+)} \mathbf{S}^* d\Omega = S^+ \quad (17a)$$

$$F^- = \iint_{\Omega(CE^-)} \mathbf{S}^* d\Omega = S^- \quad (17b)$$

The vector  $\mathbf{S}^*$  in Equations (17) is determined as follows:

- for  $CE^-$ :

$$\mathbf{S}^* = \mathbf{S}_{j-1/2}^{n-1/2} + (\mathbf{S}_x)_{j-1/2}^{n-1/2} (x - x_{j-1/2}) + (\mathbf{S}_t)_{j-1/2}^{n-1/2} (t - t^{n-1/2}) \quad (18a)$$

- for  $CE^+$ :

$$\mathbf{S}^* = \mathbf{S}_{j+1/2}^{n-1/2} + (\mathbf{S}_x)_{j+1/2}^{n-1/2} (x - x_{j+1/2}) + (\mathbf{S}_t)_{j+1/2}^{n-1/2} (t - t^{n-1/2}) \quad (18b)$$

thus

$$S^+ = \mathbf{S}_{j+1/2}^{n-1/2} \frac{\Delta x \Delta t}{4} - (\mathbf{S}_x)_{j+1/2}^{n-1/2} \frac{\Delta t (\Delta x)^2}{16} + (\mathbf{S}_t)_{j+1/2}^{n-1/2} \frac{\Delta x (\Delta t)^2}{16} \quad (19a)$$

$$S^- = \mathbf{S}_{j-1/2}^{n-1/2} \frac{\Delta x \Delta t}{4} + (\mathbf{S}_x)_{j-1/2}^{n-1/2} \frac{\Delta t (\Delta x)^2}{16} + (\mathbf{S}_t)_{j-1/2}^{n-1/2} \frac{\Delta x (\Delta t)^2}{16} \quad (19b)$$

where

$$\mathbf{S}_x = \frac{\partial \mathbf{S}}{\partial \mathbf{f}} \mathbf{f}_x \quad (20a)$$

$$\mathbf{S}_t = \frac{\partial \mathbf{S}}{\partial \mathbf{f}} \mathbf{f}_t = \frac{\partial \mathbf{S}}{\partial \mathbf{f}} \left( \mathbf{S} - \frac{\partial \mathbf{G}}{\partial x} \right) = \frac{\partial \mathbf{S}}{\partial \mathbf{f}} \left( \mathbf{S} - \frac{\partial \mathbf{G}}{\partial \mathbf{f}} \mathbf{f}_x \right) \quad (20b)$$

When there are no source terms, Equation (17) simplify to:

$$F^+ = 0 \quad (21a)$$

$$F^- = 0 \quad (21b)$$

By combining Equations (15) with Equations (17), (18) and (19) or, when source terms are absent, with Equation (21), a system of two vector equations is obtained, in which  $\mathbf{f}$  and  $\mathbf{f}_x$  are the unknowns, treated independently. All other values at the unknown time level  $n$  can be calculated as a combination of the two above values. Taking into consideration the definition of  $\mathbf{f}$ ,  $\mathbf{G}$  and  $\mathbf{S}$  in the case of the water hammer from Equation (4b), the final formulas for  $p$  and  $q$  at the unknown time level can be obtained.



The scheme presented above in its pure form, however, leads to several numerical problems. Having applied such an approach to the direct problem for the advection-diffusion equation, Chang [15] showed that in the case of pure advection, the absolute value of the amplification factor for this scheme is equal to unity, regardless of the grid size. This means that the method is always non-dissipative. In addition, accuracy analysis showed that the scheme is dispersive, and the dispersion disappears only for a Courant number equal to unity. In real-life cases, it is often difficult or impossible to perform computations with  $Cr = 1$ , and in consequence, we obtain a solution which suffers from unphysical oscillations. In order to improve the properties of this scheme, Chang [15] modified it by introducing non-zero terms (responsible for numerical dissipation) to the right-hand sides of Equations (21). The magnitude of such terms depends on the values of the derivatives at the known time level and on a numerical parameter ( $0 \leq \varepsilon \leq 1$ ), independent of any other variables. The numerical dissipation is controlled by the value of the parameter  $\varepsilon$ , which can be modified in the scheme. For  $\varepsilon = 0$ , the values of the additional terms are equal to zero (corresponding to no numerical dissipation). The terms introduced into the equations are of the same magnitude, but of opposite signs (positive for  $F^+$ , negative for  $F^-$ ). As a result, in each  $CE^+$  and  $CE^-$  cell the conservation law is not satisfied and symmetry is broken. However, the conservation law is satisfied for  $CEs$  which are sums of  $CE^+$  and  $CE^-$ , since the artificially introduced terms cancel out.

The application of the above modifications to Equation (4a) leads to:

$$\begin{aligned}
 F^+ + F^- &= \oint_{s(CE^+(j,n))} -\mathbf{G}^* dt + \mathbf{f}^* dx + \oint_{s(CE^-(j,n))} -\mathbf{G}^* dt + \mathbf{f}^* dx \\
 &= \iint_{\Omega(CE^+)} \mathbf{S}^* d\Omega + \iint_{\Omega(CE^-)} \mathbf{S}^* d\Omega = S^+ + S^-
 \end{aligned}
 \tag{22}$$

and thus:

$$\frac{2}{\Delta x} (F^+ + F^-) = \frac{2}{\Delta x} (S^+ + S^-)
 \tag{23}$$

The values of  $F^+$  and  $F^-$  are determined according to Equations (15).

After substituting the formulas for  $F^+$ ,  $F^-$ ,  $S^+$ , and  $S^-$  to Equation (22), we obtain:

$$(\mathbf{f})_j^n = \frac{1}{2} \left[ \mathbf{f}_{j-1/2}^{n-1/2} + \mathbf{f}_{j+1/2}^{n-1/2} + (\mathbf{W})_{j-1/2}^{n-1/2} - (\mathbf{W})_{j+1/2}^{n-1/2} + \mathbf{E} \right]
 \tag{24}$$

where

$$\begin{aligned}
 \mathbf{E} &= \frac{\Delta t}{8} \left\{ 4 \left[ (\mathbf{S})_{j-1/2}^{n-1/2} + (\mathbf{S})_{j+1/2}^{n-1/2} \right] + \Delta x \left[ (\mathbf{S}_x)_{j-1/2}^{n-1/2} - (\mathbf{S}_x)_{j+1/2}^{n-1/2} \right] \right. \\
 &\quad \left. + \Delta t \left[ (\mathbf{S}_t)_{j-1/2}^{n-1/2} + (\mathbf{S}_t)_{j+1/2}^{n-1/2} \right] \right\}
 \end{aligned}
 \tag{25}$$

and

$$\mathbf{s}_x = \frac{\partial \mathbf{S}}{\partial \mathbf{f}} \frac{\partial \mathbf{f}}{\partial x}, \quad \mathbf{s}_t = \frac{\partial \mathbf{S}}{\partial \mathbf{f}} \frac{\partial \mathbf{f}}{\partial t} = \frac{\partial \mathbf{S}}{\partial \mathbf{f}} \left( \mathbf{S} - \frac{\partial \mathbf{G}}{\partial x} \right)
 \tag{26}$$

The values of  $\mathbf{G}_t$ , required for the determination of  $\mathbf{W}$ , are obtained from:

$$\mathbf{G}_t = \frac{\partial \mathbf{G}}{\partial t} = \frac{\partial \mathbf{G}}{\partial \mathbf{f}} \frac{\partial \mathbf{f}}{\partial t} = \frac{\partial \mathbf{G}}{\partial \mathbf{f}} \left( \mathbf{S} - \frac{\partial \mathbf{G}}{\partial x} \right) = \frac{\partial \mathbf{G}}{\partial \mathbf{f}} \mathbf{S} - \left( \frac{\partial \mathbf{G}}{\partial \mathbf{f}} \right)^2 \frac{\partial \mathbf{f}}{\partial x} \quad (27)$$

The derivatives  $\mathbf{f}_x$  in the node  $(j, n)$  are determined according to the formula:

$$(\mathbf{f}_x)_j^n = \frac{\mathbf{f}_{j+1/2}^n - \mathbf{f}_{j-1/2}^n}{\Delta x} + (2\varepsilon - 1)(d\mathbf{f}_x)_j^n \quad (28)$$

where

$$(d\mathbf{f}_x)_j^n = \frac{(\mathbf{f}_x)_{j+1/2}^{n-1/2} + (\mathbf{f}_x)_{j-1/2}^{n-1/2}}{2} - \frac{\mathbf{f}_{j+1/2}^{n-1/2} - \mathbf{f}_{j-1/2}^{n-1/2}}{\Delta x} \quad (29)$$

and

$$\mathbf{f}_{j\pm 1/2}^n = \mathbf{f}_{j\pm 1/2}^{n-1/2} + \frac{\Delta t}{2} (f_t)_{j\pm 1/2}^{n-1/2} \quad (30)$$

The simplest approximation for  $\mathbf{f}_x$  is obtained for  $\varepsilon = 1/2$ . In this case, the formula:

$$(\mathbf{f}_x)_j^n = \frac{\mathbf{f}_{j+1/2}^n - \mathbf{f}_{j-1/2}^n}{\Delta x} \quad (31)$$

is obtained, which in fact is the central difference approximation. This formula was presented by Molls and Molls [16] without an explicit explanation to which value of  $\varepsilon$  it corresponds.

In the literature [15, 16] more involved formulas for  $\mathbf{f}_x$  can be found as well, *e.g.*:

$$(\mathbf{f}_x)_j^n = \frac{|(\mathbf{f}_{x^+})_j^n|^\omega (\mathbf{f}_{x^-})_j^n + |(\mathbf{f}_{x^-})_j^n|^\omega (\mathbf{f}_{x^+})_j^n}{|(\mathbf{f}_{x^+})_j^n|^\omega + |(\mathbf{f}_{x^-})_j^n|^\omega} \quad (32)$$

where

$$\mathbf{f}_{x^\pm} = \frac{\mathbf{f}_{j\pm 1/2}^n - \mathbf{f}_j^n}{\Delta x/2} \quad (33)$$

$\omega$  is a weighting parameter, which takes the value of either 1 or 2. For  $\omega = 0$ , the formula (30) is obtained. The application of more involved formulas for  $(\mathbf{f}_x)_j^n$ , such as Equation (32), significantly diminishes oscillations in the vicinity of the discontinuity, since the role of  $\omega$  is basically similar to that of  $\varepsilon$ .

By taking into consideration the definition of  $\mathbf{f}$ ,  $\mathbf{G}$  and  $\mathbf{S}$  from Equation (4b), final formulas for  $p$  and  $q$  at the unknown time level can be obtained. The full transition from the known time level  $(n-1)$  to the unknown level  $n$  is carried out in two steps: first, level  $(n-1/2)$  is calculated, and then (according to the same formulas) level  $n$  is obtained.

### 3. Stability and accuracy of the scheme

More information concerning any numerical features of the numerical scheme can be obtained by investigating its stability and accuracy. Usually, this

is examined for the case of a linear system of equations [20] which in the case of a water hammer can be written as follows:

$$\frac{\partial U}{\partial t} + g \frac{\partial H}{\partial x} = 0 \tag{34a}$$

$$\frac{\partial H}{\partial t} + \frac{a^2}{g} \frac{\partial U}{\partial x} = 0 \tag{34b}$$

The system of Equations (34) can be written in the form (4a), yielding:

$$\mathbf{f} = \begin{Bmatrix} U \\ H \end{Bmatrix}, \quad \mathbf{G} = \begin{Bmatrix} gH \\ \frac{a^2}{g}U \end{Bmatrix} \tag{35}$$

Formulas (25)–(30) are applied to Equation (35), and a system of algebraic equations resulting from the STC method is obtained. If the procedure is repeated twice (for both steps, *i.e.* from level  $n - 1$  to  $n - 1/2$ , and then from level  $n - 1/2$  to  $n$ ), the final system of equations with the unknowns  $\mathbf{f}_j^n$  and  $(\mathbf{f}_x)_j^n$  is obtained:

$$\mathbf{t}(j, n) = (\mathbf{P}_+)^2 \mathbf{t}(j + 1, n - 1) + (\mathbf{P}_+ \mathbf{P}_- + \mathbf{P}_- \mathbf{P}_+) \mathbf{t}(j, n - 1) + (\mathbf{P}_-)^2 \mathbf{t}(j - 1, n - 1) \tag{36}$$

where

$$\mathbf{t}(i, m) = \begin{pmatrix} U_i^m \\ \frac{\Delta x}{4} (U_x)_i^m \\ H_i^m \\ \frac{\Delta x}{4} (H_x)_i^m \end{pmatrix} \tag{37}$$

$$\mathbf{P}_+ = \frac{1}{2} \begin{bmatrix} 1 & -(1 - \text{Cr}^2) & -\frac{\Delta t g}{\Delta x} & 0 \\ 1 - \varepsilon & 2\varepsilon - 1 & 0 & -\frac{\Delta t g}{\Delta x} \\ -\frac{\Delta x}{\Delta t g} \text{Cr}^2 & 0 & 1 & -(1 - \text{Cr}^2) \\ 0 & -\frac{\Delta x}{\Delta t g} \text{Cr}^2 & 1 - \varepsilon & 2\varepsilon - 1 \end{bmatrix} \tag{38}$$

$$\mathbf{P}_- = \frac{1}{2} \begin{bmatrix} 1 & (1 - \text{Cr}^2) & \frac{\Delta t g}{\Delta x} & 0 \\ -(1 - \varepsilon) & 2\varepsilon - 1 & 0 & \frac{\Delta t g}{\Delta x} \\ \frac{\Delta x}{\Delta t g} \text{Cr}^2 & 0 & 1 & -(1 - \text{Cr}^2) \\ 0 & \frac{\Delta x}{\Delta t g} \text{Cr}^2 & -(1 - \varepsilon) & 2\varepsilon - 1 \end{bmatrix} \tag{39}$$

and  $(\mathbf{P}_+)^2 = \mathbf{P}_+ \mathbf{P}_+$ ,  $(\mathbf{P}_-)^2 = \mathbf{P}_- \mathbf{P}_-$ .

Stability analysis can be performed with use of the well-known Neumann method [21]. This is done similarly as with other applications of the STC method [15, 17]. We can conclude that:

- for  $\varepsilon \in \langle 0, 1 \rangle$  and  $\text{Cr} \leq 1$  the modulus of every eigenvalue of the amplification matrix is in the range of  $\langle 0, 1 \rangle$ , and thus the scheme is stable;
- for  $\varepsilon = 0$  and  $\text{Cr} \leq 1$  the modulus of every eigenvalue of the amplification matrix is equal to unity, which means that the wave amplitude is neither damped nor amplified and the scheme does not produce numerical diffusion;
- for  $\varepsilon \neq 0$  and  $\text{Cr} < 1$  the scheme produces numerical dissipation, whose magnitude depends on the value of  $\varepsilon$ ;
- for  $\text{Cr} = 1$  the scheme is non-dissipative, since the largest eigenvalue of the amplification matrix is equal to unity for any  $\varepsilon$ .

Additional information about numerical errors introduced by the scheme can be obtained from accuracy analysis. If all nodal values in Equation (36) are replaced with their Taylor series expansions around the node  $(j, n - 1)$ , we can obtain the modified equations, which gives us insight about the numerical errors this scheme introduces. Their analysis leads to the following conclusions:

- the scheme leads to algebraic equations that are consistent with the differential ones, as for  $\Delta x, \Delta t \rightarrow 0$ , the numerical errors tend to zero, and thus the modified equations tend to the governing system of Equations (34);
- in general, the modified equations include terms involving derivatives of the third and higher orders, which means that the scheme is of second-order accuracy, *i.e.* it generates numerical dispersion the magnitude of which is governed by the third-order derivative and numerical dissipation resulting from the fourth-order terms;
- for  $Cr = 1$  an accurate solution is obtained;
- for  $\varepsilon = 0$  even-order derivatives disappear from the right-hand sides of the modified equations, which corresponds to the absence of numerical dissipation and the presence of numerical dispersion. Numerical dispersion vanishes when  $Cr = 1$ , in which case an accurate solution is obtained.

The above conclusions result from the analysis of the linear problem. For non-linear problems, it is more difficult to estimate the magnitude of numerical dissipation and dispersion. However, according to the presented analysis, the STC method has certain advantages, particularly important when numerical errors are essential for the proper interpretation of the results.

To sum up, the most important properties of the STC method are:

- explicit formulas for  $\mathbf{f}$  and  $\mathbf{f}_x$ ;
- uniform treatment of temporal and spatial variables;
- independent determination of the values of functions and their derivatives in mesh nodes,
- small number of known values in the formula for the unknowns (thus the final formulas are relatively simple);
- global and local flux conservation (in space-time), and thus automatic enforcement of mass conservation;
- no *ad hoc* formulas for the approximation of flux;
- conditional stability ( $Cr \leq 1$ );
- dispersion and dissipation of the scheme, depending on the value of  $\varepsilon$ : no numerical diffusion for  $\varepsilon = 0$ ; for  $0 < \varepsilon \leq 1$  numerical diffusion results from the presence of terms with derivatives of the fourth order in the modified equation;
- second-order accuracy; the order of accuracy depends on the number of nodes taking part in the approximation (higher-order accuracy can be obtained by using higher-order approximations of  $\mathbf{f}^*$  and  $\mathbf{G}^*$ ).

The STC method has numerous advantages. However, it does have certain disadvantages, such as conditional stability. All in all, the analysis of its dissipative

and dispersive properties allows us to claim that it can be a good alternative to traditional methods (see *e.g.* [17]). The obtained solution suffers from very small numerical errors, and mass conservation is obeyed. This is important in many practical applications. In the case of a water hammer, this issue is essential, since it was proved that numerical errors can be a significant obstacle to the proper interpretation of the results and assessment of agreement between the measurements and calculations.

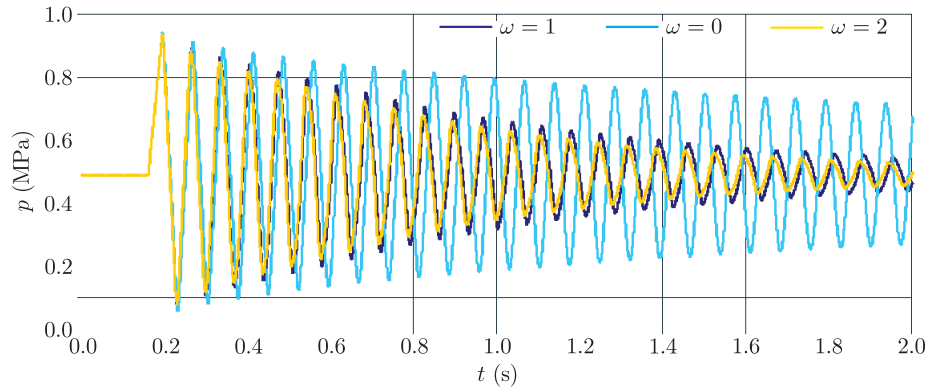
#### 4. Numerical test

The properties of the scheme can be illustrated with a classical numerical example. Let us consider a typical case of a single steel pipeline of constant diameter fed from a large pressure reservoir, in which the constant value of pressure during the experiment was enforced. The sudden closure of the valve at the downstream end of the pipeline causes rapidly varied unsteady water flow. The water hammer pressure characteristics were measured in the vicinity of the valve cross-section and calculations of pressure changes for this cross-section were performed. Here, let us consider the pipeline presented by Wichowski [22] and Weinerowska-Bords [23], for which the solutions obtained with other schemes are known. The pipeline length  $L$  is 41 m, the internal diameter  $D = 42$  mm, the wall thickness  $e = 3$  mm, the constant pressure head in the tank cross-section is 50 m, the rate of steady-state discharge  $Q_0 = 0.453$  dm<sup>3</sup>/s (velocity  $v_0 = 0.327$  m/s) and the water temperature is 4.5°C. The results of the measurements and calculations for this pipeline are presented in Figures 4–7.

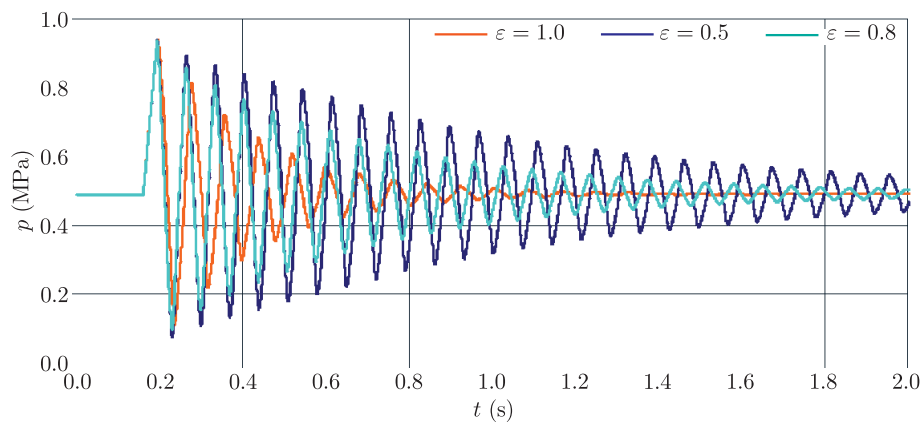
Figures 4 and 5 show the influence of the two parameters,  $\omega$  and  $\varepsilon$ , on the obtained numerical solution. Both parameters cause the damping of oscillations and strongly influence the period of the oscillations. Although, in general, the STC method is characterized by high accuracy, the modification of the numerical parameters can significantly change the numerical solution, since numerical errors, which introduce artificial dissipation and dispersion into the solutions, are inherent in all numerical modelling.

Figure 6 presents the measured pressure characteristics for the analyzed case [22]. Figure 7 presents the calculated results of the pressure in the cross-section close to the valve. The solution was obtained for  $\omega = 1$ ,  $\varepsilon = 0.55$  and a time step  $\Delta t = 0.00032$  s ( $Cr = 0.295$ ). For lower values of  $\omega$  and  $\varepsilon$  and higher values of  $\Delta t$ , the calculated results did not agree with measurements – the damping of the oscillations was too low and their frequency was either too high or too low (depending on the values of the parameters). Taking into account the relatively high accuracy of the scheme, a relatively high magnitude of the numerical error was required to yield good agreement between the calculations and measurements. However, even in such a case, the comparison between Figures 6 and 7 shows that the pressure characteristics is not satisfactorily represented. The measured pressure characteristic is smoother, while the calculated pressure characteristic is more peaked, even if the values of the local maxima and minima and the

frequency of the oscillations are similar. This confirms that the system of equations describing a water hammer does not accurately describe the phenomenon [14]. The system of equations lacks the term that would represent the mechanism of diffusion observed during the measurements.



**Figure 4.** Influence of the value of  $\omega$  on the solution of the water hammer problem ( $\varepsilon = 0.5$ ,  $Cr = 0.7$ )



**Figure 5.** Influence of the value of  $\varepsilon$  on the solution of the water hammer problem ( $\omega = 1$ ,  $Cr = 0.7$ )

## 5. Conclusions and final remarks

The presented numerical scheme can be an interesting alternative to more commonly used schemes (*e.g.* the method of characteristics, finite difference schemes, the finite volume method) used in many applications (direct and inverse problems described with a system of hyperbolic partial differential equations), including the water hammer problem. Since in its pure form the method exhibits desired numerical features (third-order accuracy in the general case, and higher orders in particular cases), it can help recognize numerical artifacts in the solution. Although a certain level of numerical dissipation is often desirable (as it can

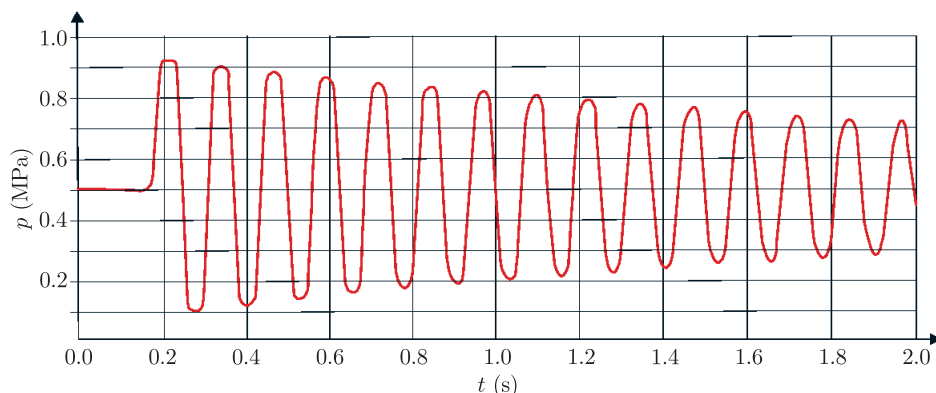


Figure 6. Measured changes in the pressure during the water hammer

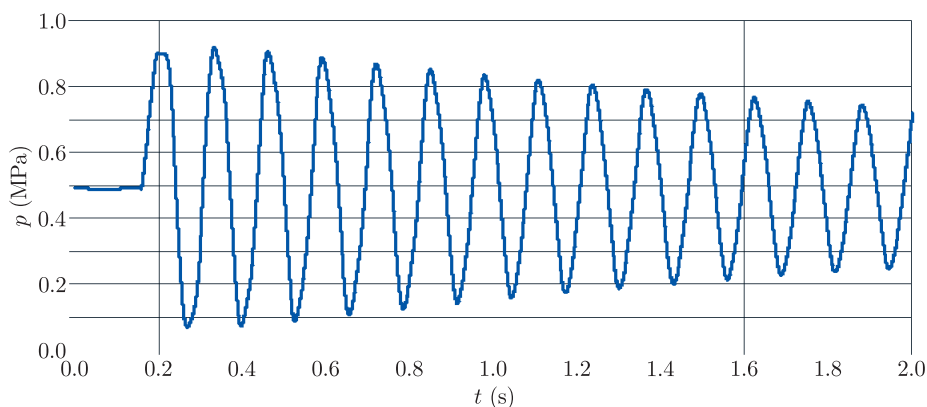


Figure 7. Calculated changes in the pressure during the water hammer (STC method,  $\omega = 1$ ,  $\varepsilon = 0.55$ ,  $Cr = 0.295$ )

improve a solution suffering from unphysical oscillations caused by numerical dispersion), too high a level of dissipation distorts the calculated results, making their interpretation very difficult.

The water hammer problem described by the system of equations (2) or (3) solved with a highly accurate scheme leads to results that do not agree well with observations. However, a solution in sufficiently good agreement with observations can be obtained by modifying the numerical parameters ( $\omega$ ,  $\varepsilon$  and  $Cr$ ). This, in fact, means that the agreement between the calculations and observations results from numerical errors incurred by the method.

### References

- [1] Allevi L 1902 *Annali della Società degli Ingegneri ed Architetti Italiani* **17** (5) 285 (in Italian)
- [2] Allevi L 1913 *Atti dell'Associazione Elettrotecnica Italiana* **17** 127 (in Italian)
- [3] Jaeger C 1933 *Le Genie Civil* **103** (26) 612 (in French)
- [4] Wood F M 1937 *Trans. ASME* **59** 707
- [5] Parmakian J 1955 *Water-Hammer Analysis*, New York, Dover Publications, Inc.

- [6] Streeter V L and Lai Ch 1962 *J. Hydr. Div. ASCE* **88** (HY3) 79
- [7] Streeter V L and Wylie E B 1967 *Hydraulic Transients*, McGraw-Hill Book Co., New York, USA
- [8] Chaudhry M H 1979 *Applied Hydr. Transients*, Van Nostrand Reinhold Company, New York
- [9] Zielke W 1968 *ASME J. Basic Eng.* **90** (1) 109
- [10] Brunone B, Golia U M and Greco M 1991 *Proc. Int. Meeting on Hydraulic Transients with Column Separation*, IAHR, Valencia, Spain, pp. 140–148
- [11] Axworthy D H, Ghidaoui M S and McInnis D A 2000 *J. Hydr. Eng. ASCE* **12** (4) 276
- [12] Silva-Araya W F and Chaundhry M H 2001 *J. Hydr. Eng.* **127** (7) 607
- [13] Ramos H, Covas D, Borga A and Loureiro D 2004 *J. Hydr. Research* **42** (4) 413
- [14] Szymkiewicz R and Mitosek M 2007 *Int. J. Numer. Meth. Fluids* **55** 1039
- [15] Chang S C 1995 *J. Comp. Phys.* **119** 295
- [16] Molls T and Molls F 1998 *J. Hydr. Eng.* **124** (5) 501
- [17] Weinerowska K 2002 *Arch. Hydro-Eng. Environ. Mech.* **49** (1) 83
- [18] Tijsseling A S and Anderson A 2007 *J. Hydr. Eng. ASCE* **1** 1
- [19] Peyret R and Taylor T D 1983 *Computational Methods for Fluid Flow*, New York, Springer-Verlag Inc.
- [20] Szymkiewicz R 2006 *The Method of the Analysis of Numerical Dissipation and Dispersion in the Solution of the Equations of Hydrodynamics*, Publication of Gdansk University of Technology, Gdansk (in Polish)
- [21] Fletcher C A J 1991 *Computational Techniques for Fluid Dynamics*, Berlin-Heidelberg, Springer-Verlag, **I**
- [22] Wichowski R 2002 *Selected Problems of Unsteady Flow in Looped Water Distribution Systems*, Publication of Gdansk University of Technology, Monography, Gdansk **27** (in Polish)
- [23] Weinerowska-Bords K 2007 *TASK Quart.* **11** (4) 383